Hydrogen Sensing Using Thin-Film Perfect Light Absorber

Mohamed ElKabbash,*,[†,‡] Kandammathe V. Sreekanth,[†] Yunus Alapan,[§] Myeongseop Kim,[§] Jonathan Cole,[∥] Arwa Fraiwan,[§] Theodore Letsou,[†] Yandong Li,[†] Chunlei Guo,[‡,⊥] R. Mohan Sankaran,[∥] Umut A. Gurkan,[§,#,○,□] Michael Hinczewski,[†] and Giuseppe Strangi*,[†,△,○]

[†]Department of Physics, Case Western Reserve University, 10600 Euclid Avenue, Cleveland, Ohio 44106, United States

[‡]The Institute of Optics, University of Rochester, Rochester, New York 14627, United States

[§]Case Biomanufacturing and Microfabrication Laboratory, Mechanical and Aerospace Engineering Department, Case Western Reserve University, Cleveland, Ohio 44106, United States

[∥]Department of Chemical and Biomolecular Engineering, Case Western Reserve University, Cleveland, Ohio United States

[⊥]GPL, State Key Laboratory of Applied Optics, Changchun Institute of Optics, Fine Mechanics and Physics, Chinese Academy of Sciences, Changchun 130033, China

[#]Biomedical Engineering Department, Case Western Reserve University, Cleveland, Ohio 44106, United States

[○]Department of Orthopedics, Case Western Reserve University, Cleveland, Ohio 44106, United States

[□]Advanced Platform Technology Center, Louis Stokes Cleveland Veterans Affairs Medical Center, Cleveland, Ohio 44106, United States

[△]CNR-NANOTEC, Istituto di Nanotecnologia and Department of Physics, University of Calabria, Rende CS, Italy

[○]Istituto Italiano di Tecnologia, Via Morego 30, 16163, Genova, Italy

S *Supporting Information*
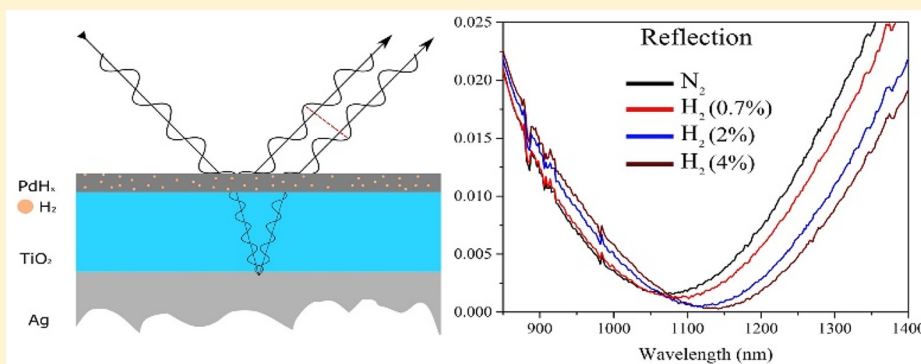
ABSTRACT: Hydrogen sensing is important in many industrial, biomedical, environmental, and energy applications. Realizing a practical, reliable, and inexpensive hydrogen sensor, however, is an ongoing challenge. Here, we demonstrate hydrogen sensing based on an optically active metal−dielectric−metal (MDM) perfect light absorber. The cavity enables perfect broadband light absorption (>99.999%) with optical losses localized in an ultrathin palladium (Pd) layer. Upon exposure to hydrogen, the Pd layer forms a hydride which actively shifts the cavity minimum reflectance wavelength by ∼60 nm for a hydrogen concentration of 4%. The sensor enjoys extremely high figure of merit. The ease of fabrication, large area, and high sensitivity of our sensor make it an attractive and practical option, especially for miniaturized hydrogen sensors vital for medical and food safety applications.

KEYWORDS: thin films, Fabry-Perot cavity, interference, gas sensing, hydrogen sensing, nanophotonics

Hydrogen is highly flammable with low ignition energy at ambient temperature and pressure and concentrations ranging from 4 to 75%.[1] Consequently, hydrogen sensing is an important safety issue in industries where it is a crucial component or a byproduct. Gas chromatography and mass spectrometry systems are suitable for large scale industrial sensing; however, they may not be suitable for applications that require miniaturization, for example, detection of hydrogen in the breath that can indicate various diseases, such as lactose intolerance, and detection of hydrogen produced by bacteria in food industries.[2−4] Several nanophotonic and plasmonic systems have been reported for optical-based hydrogen sensing.[5,6] Nanophotonic and plas-
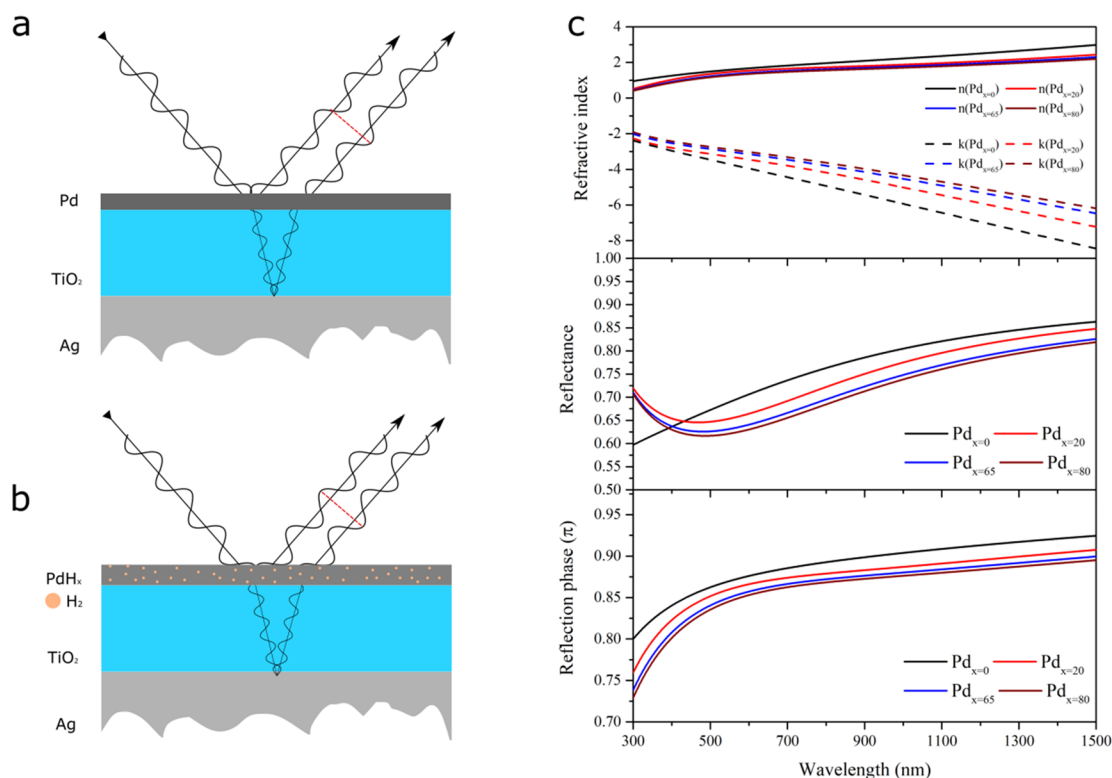
Figure 1. Sensing mechanism: (a) A schematic illustration of the MDM sensor consisting of a Pd−TiO$_2$−Ag thin film stack. The reflection is decreased via destructive interference. (b) By introducing hydrogen, the Pd film converts into a hydride PdH$_x$ with a hydrogen stoichiometry (x). The MDM cavity is designed such that the formation of a hydride fully suppresses reflection and PLA is realized. (c) The real (n) and imaginary (k) components of Pd at various hydrogen atomic ratios (0, 20, 65, and 80%) are shown in the top panel. The middle panel shows the reflectance from a bulk Pd substrate at the same hydrogen stoichiometry. The bottom panel shows the reflection phase at an air−Pd interface for the different hydrogen atomic ratios.

monic materials enable the control of light at the subwavelength scale.[5] In particular, metals that form metal hydrides, for example, palladium (Pd), are used for optical hydrogen sensors as they provide strong optical and electronic response to hydrogen. Upon exposure to hydrogen, Pd forms a hydride (PdH$_x$), which can form a solid solution (α phase) at low hydrogen partial pressure or a solid hydride phase (β phase) at higher hydrogen partial pressure.[7] In the β phase, the lattice parameter increases by ∼3.5% as the lattice expands to accommodate the hydrogen atoms occupying new lattice sites.[7] At intermediate hydrogen partial pressures, both α and β phases coexist in a Pd film (so-called α' phase).[8] The change in the complex permittivity and lattice structure of Pd provides a detectable optical response from a photonic[9] or a plasmonic[2,5,6] sensor.

While metal hydride photonic sensors are relatively selective,[10] they require lithography to fabricate, which is high cost, low throughput, and prone to imperfections, an impediment to commercialization of hydrogen sensors.[11,12] Hydrogen sensing based on light absorption using Pd nanograting on a multilayer system was introduced by Tittl et al.[5] The reflection was suppressed by matching the impedance of free space to achieve perfect light absorption (PLA; ∼99.5%). The change in Pd nanograting complex refractive index red-shifted the absorption maximum $\Delta\lambda_{max} \approx$ 19 nm and a change in the figure of merit (FOM $\equiv \Delta R/R$) of up to 500. On the other hand, realizing perfect light absorption using thin-film stack of metals, dielectrics, and semiconductors, has been demonstrated using different geometries.[13,14] Thin

film light absorbers represent an inexpensive and scalable alternative that enables many applications, for example, structural coloring,[15] solar thermal energy applications,[16,17] water splitting,[18] photocatalysis,[19] polarizers,[20] and heat-assisted magnetic recording.[21]

In this work, we experimentally demonstrate hydrogen sensing using a thin-film perfect light absorber as a scalable and lithography-free hydrogen sensor. The perfect light absorber consists of a metal-dielectric-metal nanocavity with Pd as a top metal layer. Perfect light absorption is realized via amplitude splitting destructive interference and the strong optical losses inside Pd. The cavity's resonance is sensitive to Pd optical properties, which undergoes significant changes when exposed to hydrogen. At 4% hydrogen concentration, the cavity's resonance red shifts by 60 nm. The fabrication simplicity and sensitivity of our sensor make it a promising candidate for practical hydrogen sensing applications. More importantly, the sensor provides a significant red shift of ∼15 nm at a low hydrogen concentration of 0.7%.[12]

To realize perfect light absorption, light should be critically coupled to the absorber.[22,23] Critical light coupling occurs when absorption equals the sum of the reflection, transmission, and scattering. For opaque metallic susbtrates in the order of 100 nm, the transmission is ∼0. In addition, scattering can be ignored for smooth thin films. To critically couple light to a thin film cavity, it is necessary and sufficient to balance absorption and reflection. Using amplitude-splitting destructive interference, reflection can be suppressed in thin films,[16] such that light is entirely trapped inside the resonator and is
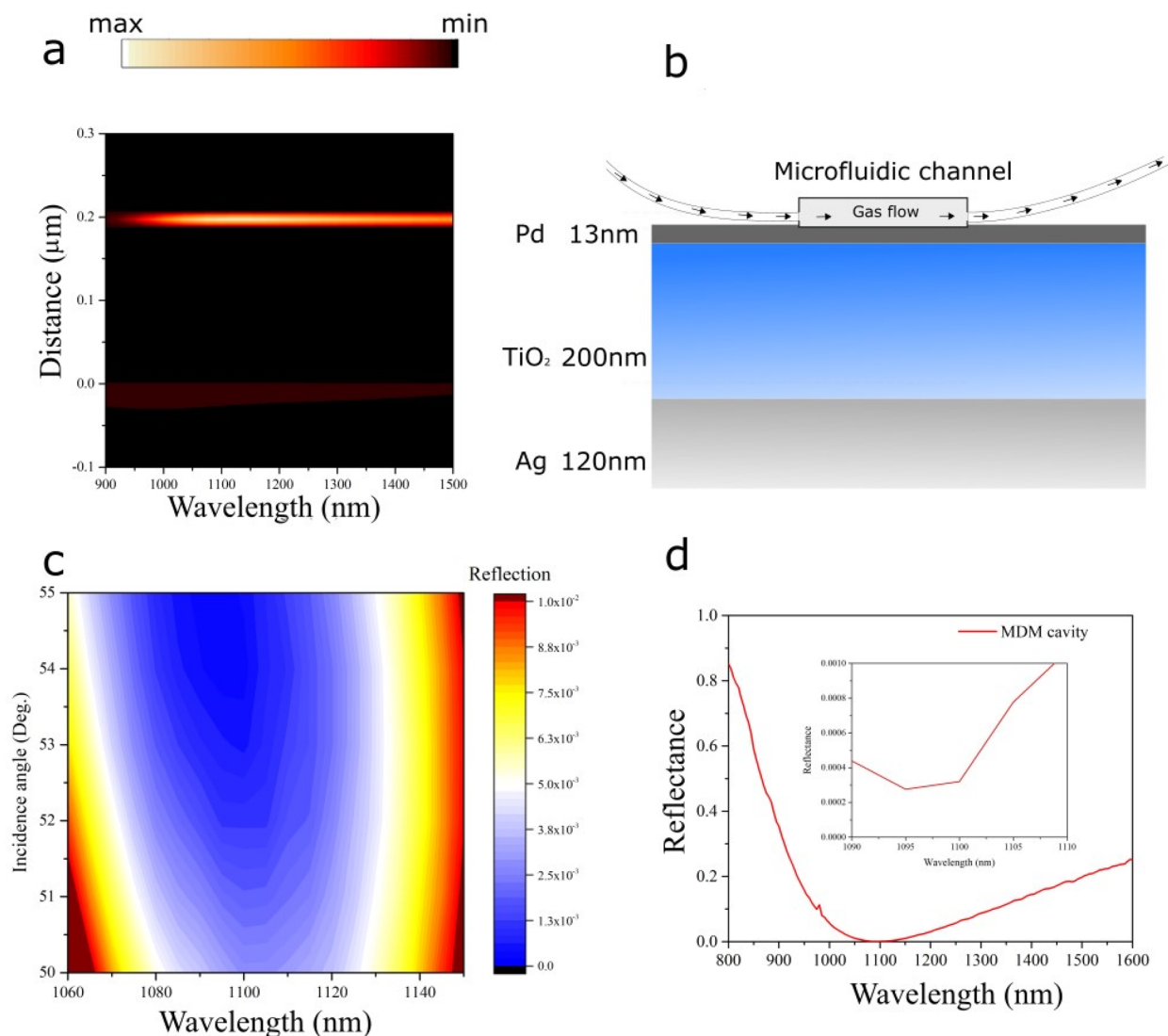
Figure 2. Perfect light absorption in Pd−TiO$_2$−Ag cavity. (a) FDTD calculation of the optical power density dissipated inside the cavity showing that the density of optical losses inside the Pd film is an order of magnitude higher than that occurring inside the Ag film, which behaves as a PEC for longer wavelengths. (b) A schematic of the Pd (13 nm)−TiO$_2$ (200 nm)−Ag (120 nm) thin-film cavity with a microfluidic channel added on top where the gas flows and interact with the sample. (c) The measured angular reflection measurements to determine the angle at which perfect light absorption takes place. (d) Reflectance of the fabricated cavity at 54° incidence angle for the bare sample showing perfect light absorption at ~1100 nm.

dissipated due to the existence of losses. To achieve PLA the interfering waves must be out of phase (the phase condition), and the out-of-phase waves must be of equal amplitude (the amplitude condition).[13] Consequently, light is trapped inside a lossy medium and is eventually dissipated entirely. In an MDM cavity, it is straightforward to satisfy the amplitude condition since the metal layers are highly reflective and the incident field amplitude is split between them. Consequently, changes in the reflectance of any of the metal films would modify the amplitude condition and the magnitude of light absorption.[11,16] Assuming that both metal films behave as a perfect electric conductor (PEC), the phase condition is realized when the optical thickness of the dielectric $t_{Opt} \equiv n_d t = m\lambda/2$, where n_d and t are the refractive index and thickness of the dielectric film, respectively, and m is an integer. However, if the metal films do not behave as a PEC, the films introduce a nontrivial phase shift, that is, $\Delta\varnothing \neq 0, \pi$, which modifies the cavity resonant wavelength for a given t_{Opt}.

The operation principle of the MDM hydrogen sensor is depicted in Figure 1a,b, where the reversible transformation of Pd to Pd$_x$ changes the cavity resonance wavelength due to changes in the Pd optical constants. As shown in Figure 1c, top panel, the real (n) and imaginary (k) components of Pd complex refractive index change significantly as the hydrogen atomic ratio x increases from 0 to 80%. Clearly, the difference in the complex refractive indices between Pd and Pd hydrides increase for longer wavelengths. Consequently, operating the sensor at longer wavelengths leads to higher sensitivity. The change in refractive index significantly changes the reflection of Pd, as shown in Figure 1c, middle panel, which directly affects the magnitude of light absorption in MDM cavities. Furthermore, the phase of reflected light from an air−Pd interface change considerably as a function of hydrogen atomic ratio (stoichiometry), which would change the wavelength at which the phase condition is satisfied.
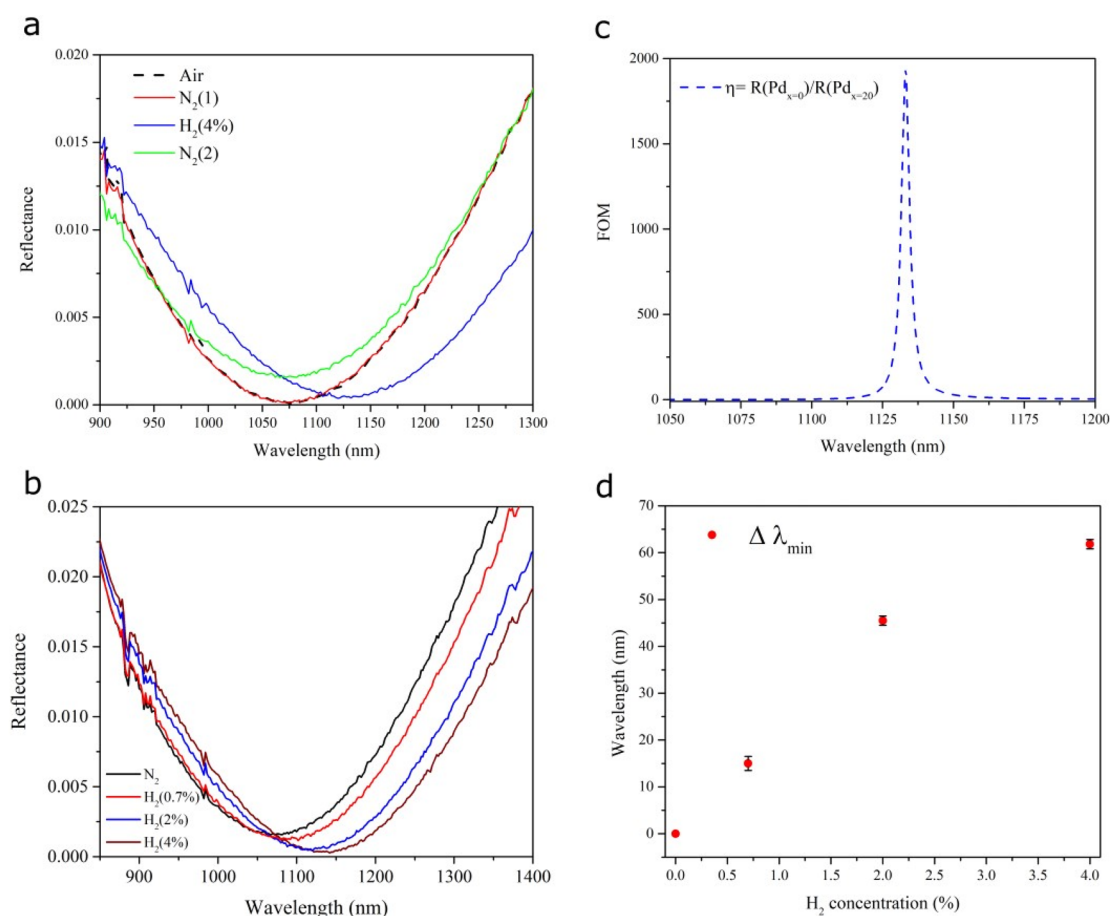
Figure 3. Reflectance with varying hydrogen concentration: (a) The measured reflection of the MDM absorber before and after introducing hydrogen. (b) The absorption mode red-shifts and absorptance increases by increasing the hydrogen concentration. (c) Calculated FOM (η) for the MDM cavity used based on the obtained optical constants of Pd and $PdH_{x=20}$. (d) The measured $\Delta\lambda_{min}$ as a function of hydrogen concentration.

The sensor consisted of a 13 nm Pd−200 nm TiO_2−120 nm Ag MDM cavity. The ultrathin thickness of the Pd layer ensures the sensor's reliability. This is because for Pd films with thickness < 20 nm, Pd films do not suffer from mechanical deformation upon forming a hydride due to the reduced tensile stiffness in thinner films.[24] The dielectric thickness is chosen to be 200 nm so that the cavity resonance lies in the NIR at a wavelength with high transmission within the atmospheric window. Indeed, operating at longer wavelengths (1700 and 2100 nm) lead to higher sensitivity (see Supporting Information, Figures S1 and S2). However, at these wavelengths, light is strongly attenuated by water vapor and remote optical sensing with adequate signal intensity may not be possible. The power dissipation density of normally incident plane waves on the fabricated MDM cavity was calculated using the commercially available finite-difference time-domain software from Lumerical. As shown in Figure 2a, the power dissipation density inside the Pd layer is an order of magnitude higher than that inside the Ag film since Pd has significantly higher optical absorption. Note that, for longer wavelengths, the Ag film approaches the PEC condition such that the field penetration and, consequently, the power dissipated/decreased. The strong localization of light absorption in the Pd layer ensures that the cavity's absorption properties will modify strongly due to slight changes in the Pd film optical

properties.[25] Hence, the MDM cavity sensor is expected to exhibit high sensitivity.

A schematic of the sensor is shown in (Figure 2b). The MDM cavity was deposited on a glass slide. Pd and TiO_2 were deposited by electron beam evaporation at a rate of 0.5 Å·s^{-1}, while Ag was deposited using thermal evaporation at 20 Å·s^{-1}. A microfluidic channel comprised of a poly(methyl methacrylate) (PMMA) plastic top (encompassing laser micromachined inlets and outlets) and a double-sided 100 μm adhesive film defining the outlines and thickness of the microchannels was added to the top of the sensor. To expose the sensor to different hydrogen concentrations, the channel inlet was connected to a tank of nitrogen mixed with 4% volume concentration H_2 and another with pure nitrogen. The gas flow from both tanks was controlled separately using two mass flow controllers (MFCs). By adjusting the MFCs, we could control the hydrogen concentration (between 0 and 4%) introduced to the sample. The sensor was then placed on a variable angle ellipsometer (J. A. Wollam, V-VASE) to measure the reflectivity R as a function of angle of incidence.

The measured angular reflection of the bare sensor, that is, without the channel, is shown in Figure 2c. We determined the operation angle by choosing the angle at which reflection is minimized. As shown in Figure 2d, we obtain perfect light absorption at 54° (see Supporting Information, Figure S3). At this angle, the measured reflectance at 1095 nm is 0.0002.

Introducing the channel, however, affects the measured reflectivity as it splits the incident beam into two reflected beams. We investigated the beam reflected from the sensor surface from, which we can determine the reflection minimum of the cavity mode.

As shown in Figure 3a, after introducing pure N_2 to the sensor, we do not see any shift in the reflection minimum at λ_{min} (red curve) compared to the reflectance measured when the sample is exposed to ambient air (dashed black curve). In comparison, after introducing N_2 mixed with 4% of H_2, we see a clear red shift in the reflection minimum as well as a change in the reflection amplitude due to the intercalation of hydrogen atoms in the Pd lattice as expected.[2] By introducing pure N_2 to the channel again, the reflection mode blue shifts. However, the absorption properties of the pure Pd film has now permanently changed. This is likely due to lattice adjustments in the thin Pd film due to strains associated with adsorbing and releasing hydrogen molecules. The following cycles of introducing N_2 mixed with 4% of H_2, and pure N_2, show no change in the spectral properties of the absorption mode. An important figure of merit (FOM) that can capture the optical activity of our absorber is $\eta = R\left(Pd_0\right)/R\left(Pd_x\right)$, where $R\left(Pd_0\right)$ is the reflectivity of the sensor without hydrogen and $R\left(Pd_x\right)$ is the reflectivity of the sensor for Pd hydride with hydrogen stoichiometry x. However, because the microfluidic channel reduces the sample reflection for most wavelengths, it is difficult to assess the true reflectance of the sample. In Figure 3b, we show the calculated FOM for our sensor containing a hydride with a hydrogen stoichiometry 20%, that is, $R\left(Pd_0\right)/R\left(Pd_{20}\right)$, is ~2000, which is significantly higher than that obtained in previous works (see Methods).[5] In fact, the FOM was found to be orders of magnitude higher for particular configurations. As an example of the extremely high FOM that can be obtained from MDM hydrogen sensor, the calculated FOM of an MDM cavity comprised of Pd (5.91 nm)−TiO_2 (200 nm)−Ag (60 nm), λ_{min} = 1506 nm at incident angle = 40° is 924363.

We also studied the total spectral shift in λ_{min} for different hydrogen concentrations. Practical hydrogen sensors must be able to respond to hydrogen at concentrations approximately an order of magnitude lower than the explosive limit of H_2 (4%).[12] As shown in Figure 3c, λ_{min} shifts gradually for various hydrogen concentrations. The total λ_{min} shift is 15, 45.5, and 62 nm, for hydrogen concentrations of 0.7, 2, and 4%, respectively (see Figure 3d).

In summary, we have demonstrated a large-area, lithographically free hydrogen gas sensor based on palladium-based thin-film perfect light absorber. The MDM cavity is sensitive to modification in the absorption and reflection phase properties of Pd. The strong absorption in the Pd layer and the strong modification in the refractive index of and reflection phase from hydrogenated-Pd resulted in extreme hydrogen sensitivity. The λ_{min} shift is significantly higher than what was previously reported using a perfect absorber.[5] Future work can realize perfect light absorption in the visible range to enable monitoring hydrogen by looking at color changes, as predicted numerically in ref 26, which is a similar result to the work by Ngene et al.[10]

■ METHODS

Cavity Fabrication. To fabricate the thin film absorber, we first cleaned glass slides (Micro slides, Corning) with acetone solution then dried the slides. A total of 120 nm of Ag was deposited using thermal evaporation at 5 nm·s^{-1} deposition rate. A total of 200 nm of TiO_2 and 13 nm of Pd were then deposited using electron beam evaporation at 0.2 Å·s^{-1} and a base pressure of <5 × 10^{-6} mbar.

Microfluidic Channel Fabrication. The microfluidic channel consists of a poly(methyl methacrylate) plastic top (encompassing micromachined inlets and outlets) and a double-sided adhesive film defining the outlines and thickness of the microchannels. PMMA tops with inlets and outlets were laser micromachined (diameter 0.61 mm, separation 12.4 mm) using a VersaLASER system (Universal Laser Systems). A double-sided adhesive film (iTapestore, 100 μm in height) was laser cut in the same size of PMMA tops and 14 × 2 mm microchannels within. The film was attached to the PMMA component to include the inlet and outlet between the outline of the channels. Fluorinated ethylene propylene (FEP) tubing (Cole-Parmer) was used to connect the gas sources to the microchannels. Tubing and all connections to the tubing, between gas sources and channel, was sealed using a 5 min epoxy (Devcon). A picture of the actual sensor is shown in Supporting Information, Figure S4.

Angular Reflection Measurements. Angular reflection was measured using Variable-angle high-resolution spectroscopic ellipsometer (J. A. Woollam Co., Inc., V-VASE). The transmittance is 0 for all wavelengths and angles. Since we are dealing with thin films, perfect light absorption corresponds to near zero reflectance. While the maximum resolution of the ellipsometer is 0.03 nm, the measurements were taken with a resolution of 1 nm. The additional beam reflected from the microfluidic channel is blocked by the ellipsometer detector's iris.

Materials Optical Constants and FOM Calculation. The optical constants for TiO_2 and Ag used in the calculations were obtained by fitting the Wemple-DiDomenico[27] and Drude dielectric models, respectively, to single-layer ellipsometry data for each material. The optical constants for Pd_x were based on the experimental results by Vargas et al.,[28] which were fit to a Brendel−Bormann dielectric model.[29−31] From the obtained optical constants of PdH_x, we were able to calculate the FOM using transfer matrix method calculations following Chilwell and Hodgkinson.[32]

Numerical Simulations. The calculated power dissipation distribution in the thin-film stack was performed using the commercially available finite-difference, time-domain software from Lumerical. The simulation was performed using a 2D model with incident plane wave. The mesh was tailored to each layer with a mesh step of 0.001 nm for the Pd layer and 0.005 nm for the rest of the structure.

■ ASSOCIATED CONTENT

Ⓢ Supporting Information

The Supporting Information is available free of charge on the ACS Publications website at DOI: 10.1021/acsphotonics.9b00764.

> Reflection measurements of hydrogen sensors operating in the IR, angular reflection measurements for the sensor, and a photo of the actual sensor (PDF)

■ AUTHOR INFORMATION

Corresponding Authors
*E-mail: mke23@case.edu.
*E-mail: gxs284@case.edu.

ORCID ⊙

Mohamed ElKabbash: 0000-0003-3795-7714
R. Mohan Sankaran: 0000-0002-9399-4790

Notes

The authors declare no competing financial interest.

■ REFERENCES

(1) Fong, N. R.; Berini, P.; Tait, R. N. Hydrogen sensing with Pd-coated long-range surface plasmon membrane waveguides. *Nanoscale* **2016**, *8*, 4284−4290.

(2) Wadell, C.; Syrenova, S.; Langhammer, C. Plasmonic Hydrogen Sensing with Nanostructured Metal Hydrides. *ACS Nano* **2014**, *8*, 11925−11940.

(3) Wilkins, J. R.; Stoner, G. E.; Boykin, E. H. Microbial detection method based on sensing molecular hydrogen. *Appl. Microbiol.* **1974**, *27*, 949−952.

(4) Hitchcock, C. H. S. Determination of Hydrogen as a Marker in Irradiated Frozen Food. *J. Sci. Food Agric.* **2000**, *80*, 131−136.

(5) Tittl, A.; Mai, P.; Taubert, R.; Dregely, D.; Liu, N.; Giessen, H. Palladium-Based Plasmonic Perfect Absorber in the Visible Wavelength Range and Its Application to Hydrogen Sensing. *Nano Lett.* **2011**, *11*, 4366−4369.

(6) Liu, N.; Tang, M. L.; Hentschel, M.; Giessen, H.; Alivisatos, A. P. Nanoantenna-enhanced gas sensing in a single tailored nanofocus. *Nat. Mater.* **2011**, *10*, 631.

(7) Syrenova, S.; Wadell, C.; Nugroho, F. A. A.; Gschneidtner, T. A.; Diaz Fernández, Y. A.; Nalin, G.; Świtlik, D.; Westerlund, F.; Antosiewicz, T. J.; Zhdanov, V. P.; Moth-Poulsen, K.; Langhammer, C. Hydride formation thermodynamics and hysteresis in individual Pd nanocrystals with different size and shape. *Nat. Mater.* **2015**, *14*, 1236.

(8) Manchester, F. D.; San-Martin, A.; Pitre, J. M. The H-Pd (Hydrogen-Palladium) System. *J. Phase Equilib.* **1994**, *15*, na.

(9) Zhao, Y.; Wu, Q.; Zhang, Y. High-Sensitive Hydrogen Sensor Based on Photonic Crystal Fiber Model Interferometer. *IEEE Trans. Instrum. Meas.* **2017**, *66*, 2198−2203.

(10) Ngene, P.; Radeva, T.; Slaman, M.; Westerwaal, R. J.; Schreuders, H.; Dam, B. Seeing Hydrogen in Colors: Low-Cost and Highly Sensitive Eye Readable Hydrogen Detectors. *Adv. Funct. Mater.* **2014**, *24*, 2374−2382.

(11) Li, Z.; Butun, S.; Aydin, K. Large-Area, Lithography-Free Super Absorbers and Color Filters at Visible Frequencies Using Ultrathin Metallic Films. *ACS Photonics* **2015**, *2*, 183−188.

(12) Pitts, R.; P, L, Lee, S.-H.; Tracy, E. Interfacial Stability of Thin Film Hydrogen Sensors. *Proceedings of the 2001 DOE Hydrogen Program Review*, 2001; https://www.energy.gov/eere/fuelcells/downloads/proceedings-2001-us-doe-hydrogen-program-review.

(13) Kats, M. A.; Capasso, F. Optical absorbers based on strong interference in ultra-thin films. *Laser & Photonics Reviews* **2016**, *10*, 735−749.

(14) Sreekanth, K. V.; ElKabbash, M.; Caligiuri, V.; Singh, R.; De Luca, A.; Strangi, G. *New Directions in Thin Film Nanophotonics*; Springer: Singapore, Singapore, 2019; Vol. *1*.

(15) Letsou, T.; ElKabbash, M.; Iram, S.; Hinczewski, M.; Strangi, G. Heat-induced perfect light absorption in thin-film metasurfaces for structural coloring [Invited]. *Opt. Mater. Express* **2019**, *9*, 1386−1393.

(16) ElKabbash, M.; Iram, S.; Letsou, T.; Hinczewski, M.; Strangi, G. Designer Perfect Light Absorption Using Ultrathin Lossless Dielectrics on Absorptive Substrates. *Adv. Opt. Mater.* **2018**, *6*, 1800672.

(17) ElKabbash, M.; Sousa-Castillo, A.; Nguyen, Q.; Mariño-Fernández, R.; Hoffman, N.; Correa-Duarte, M. A.; Strangi, G. Tunable Black Gold: Controlling the Near-Field Coupling of Immobilized Au Nanoparticles Embedded in Mesoporous Silica Capsules. *Adv. Opt. Mater.* **2017**, *5*, 1700617.

(18) Dotan, H.; Kfir, O.; Sharlin, E.; Blank, O.; Gross, M.; Dumchin, I.; Ankonina, G.; Rothschild, A. Resonant light trapping in ultrathin films for water splitting. *Nat. Mater.* **2013**, *12*, 158.

(19) Song, H.; Wu, W.; Liang, J.-W.; Maity, P.; Shu, Y.; Wang, N. S.; Mohammed, O. F.; Ooi, B. S.; Gan, Q.; Liu, D. Ultrathin-Film Titania Photocatalyst on Nanocavity for CO2 Reduction with Boosted Catalytic Efficiencies. *Global Challenges* **2018**, *2*, 1800032.

(20) Sreekanth, K. V.; ElKabbash, M.; Medwal, R.; Zhang, J.; Letsou, T.; Strangi, G.; Hinczewski, M.; Rawat, R. S.; Guo, C.; Singh, R., Generalized Brewster Angle Effect in Thin-Film Optical Absorbers and Its Application for Graphene Hydrogen Sensing. *ACS Photonics* **2019**.61610

(21) Deng, C.; Song, H.; Parry, J.; Liu, Y.; He, S.; Xu, X.; Gan, Q.; Zeng, H. Nanocavity induced light concentration for energy efficient heat assisted magnetic recording media. *Nano Energy* **2018**, *50*, 750−755.

(22) ElKabbash, M.; Ilker, E.; Letsou, T.; Hoffman, N.; Yaney, A.; Hinczewski, M.; Strangi, G. Iridescence-free and narrowband perfect light absorption in critically coupled metal high-index dielectric cavities. *Opt. Lett.* **2017**, *42*, 3598−3601.

(23) Tischler, J. R.; Bradley, M. S.; Bulović, V. Critically coupled resonators in vertical geometry using a planar mirror and a 5 nm thick absorbing film. *Opt. Lett.* **2006**, *31*, 2045−2047.

(24) Lee, E.; Lee, J. M.; Koo, J. H.; Lee, W.; Lee, T. Hysteresis behavior of electrical resistance in Pd thin films during the process of absorption and desorption of hydrogen gas. *Int. J. Hydrogen Energy* **2010**, *35*, 6984−6991.

(25) Song, H.; Guo, L.; Liu, Z.; Liu, K.; Zeng, X.; Ji, D.; Zhang, N.; Hu, H.; Jiang, S.; Gan, Q. Nanocavity Enhancement for Ultra-Thin Film Optical Absorber. *Adv. Mater.* **2014**, *26*, 2737−2743.

(26) Serhatlioglu, M.; Ayas, S.; Biyikli, N.; Dana, A.; Solmaz, M. E. Perfectly absorbing ultra thin interference coatings for hydrogen sensing. *Opt. Lett.* **2016**, *41*, 1724−1727.

(27) Wemple, S. H.; DiDomenico, M. Behavior of the Electronic Dielectric Constant in Covalent and Ionic Materials. *Phys. Rev. B* **1971**, *3*, 1338−1351.

(28) Vargas, W. E.; Rojas, I.; Azofeifa, D. E.; Clark, N. Optical and electrical properties of hydrided palladium thin films studied by an inversion approach from transmittance measurements. *Thin Solid Films* **2006**, *496*, 189−196.

(29) Brendel, R.; Bormann, D. An infrared dielectric function model for amorphous solids. *J. Appl. Phys.* **1992**, *71*, 1−6.

(30) Rakić, A. D.; Djurišić, A. B.; Elazar, J. M.; Majewski, M. L. Optical properties of metallic films for vertical-cavity optoelectronic devices. *Appl. Opt.* **1998**, *37*, 5271−5283.

(31) Vargas, W. E.; Azofeifa, D. E.; Clark, N.; Solis, H.; Montealegre, F.; Cambronero, M. Parametric formulation of the dielectric function of palladium and palladium hydride thin films. *Appl. Opt.* **2014**, *53*, 5294−5306.

(32) Chilwell, J.; Hodgkinson, I. Thin-films field-transfer matrix theory of planar multilayer waveguides and reflection from prism-loaded waveguides. *J. Opt. Soc. Am. A* **1984**, *1*, 742−753.